Journal of Alloys and Compounds 722 (2017) 138–144

Contents lists available at ScienceDirect

Journal of Alloys and Compounds

journal homepage: http://www.elsevier.com/locate/jalcom

Fabrication of Al–35Zn alloys with excellent damping capacity and mechanical properties

H.J. Jiang [a], C.Y. Liu [a, b, *], Z.Y. Ma [b, **], X. Zhang [c], L. Yu [a], M.Z. Ma [c], R.P. Liu [c]

[a] Key Laboratory of New Processing Technology for Nonferrous Metal & Materials, Ministry of Education, Guilin University of Technology, Guilin, 541004, China
[b] Shenyang National Laboratory for Materials Science, Institute of Metal Research, Chinese Academy of Sciences, 72 Wenhua Road, Shenyang, 110016, China
[c] State Key Laboratory of Metastable Materials Science and Technology, Yanshan University, Qinhuangdao, 066004, China

ARTICLE INFO

Article history:
Received 17 April 2017
Received in revised form
2 June 2017
Accepted 7 June 2017
Available online 8 June 2017

Keywords:
Al alloy
Rolling
Damping capacity
Mechanical properties

ABSTRACT

In this study, rolling was performed on a binary Al–35Zn alloy. The grain refinement and dynamic precipitation were obtained in the rolled samples. The nano-sized Zn phase with a rod-like shape was obtained in the hot rolled sample, whereas the precipitated Zn phases were coarsened to hundreds nanometer with an equiaxed shape and located at the triple junctions of the Al grains after cold rolling. The cold rolled sample exhibited excellent damping capacity, mainly attributed to the special microstructure characterized by fine grains, low solid solubility, and wetting interface between Al and Zn phases. Furthermore, the cold rolled sample showed a ductile fracture and high ultimate tensile strength, with the main strengthening mechanisms being dislocation and boundary strengthening. The hot rolled sample with 90% reduction showed balanced mechanical properties, including high strength and reasonable ductility. This work provided an effective strategy of preparing Al alloys with excellent damping capacity and mechanical properties.

1. Introduction

Damping and mechanical properties are two important factors in the design of the structure materials in modern industries [1]. Al alloys are widely used in aircraft, aerospace and defense applications because of their excellent mechanical properties [2]. However, Al alloys usually exhibit low damping capacity, which limits their engineering applications in some fields.

In previous studies, it was reported that the damping capacities of Al alloys could be improved by adding high-density macroscopic pores [3] and high damping particles with a large size [4–8]. However, the mechanical properties of Al alloys such as tensile strength or ductility are inevitably deteriorated by the pores and such particles. So, obtaining a good combination of the mechanical properties and damping capacities has become a critical challenge for the engineering applications of Al alloys.

According to the current internal friction theory, the damping mechanism of Al alloys could be divided to dislocation damping and interfacial damping [9–11]. The dislocation damping mechanism is based on Granato–Lücke model [12]. In this case, the damping behavior is related with the dislocation movement and interaction between dislocations and pinning points such as solute atoms, vacancies and precipitates [13,14]. Reducing the number of solute atoms and precipitates can increase the damping capacity of Al alloys. However, Al alloys with above structural characteristics always exhibit a poor mechanical property due to the low solid solution and precipitation strengthening effects.

For the interfacial damping mechanism, the damping capacity of Al alloys is mainly controlled by the phase boundary (PB) or grain boundary (GB) sliding behaviors. It is well documented that improvement of the PB or GB sliding capacity can increase the damping capacity of Al alloys [10,15] and high PB/GB sliding capacity usually corresponds to the well mechanical properties of Al alloys [16–19]. Phase/grain refinement and PB/GB structure optimization can effectively optimize the PB/GB sliding behaviors of Al alloys, and therefore improve the damping capacity of Al alloys without sacrificing their mechanical properties.

* Corresponding author. Key Laboratory of New Processing Technology for Nonferrous Metal & Materials, Ministry of Education, Guilin University of Technology, Guilin, 541004, China.
** Corresponding author. Shenyang National Laboratory for Materials Science, Institute of Metal Research, Chinese Academy of Sciences, Shenyang, 110016, China
E-mail addresses: lcy261@glut.edu.cn (C.Y. Liu), zyma@imr.ac.cn (Z.Y. Ma).

http://dx.doi.org/10.1016/j.jallcom.2017.06.091
0925-8388/

Zn–22 wt.% Al eutectoid alloy exhibits high damping capacity due to the well Al/Zn phases sliding capacity which can be explained by the diffusive flux on the boundaries between Al and Zn phases [15,20,21]. It is discovered that the similar microstructure with coexistence of equiaxed Al and Zn phases could be also obtained in the Al–Zn alloys with lower Zn concentration after solid solution treatment and deformation [22–26]. Our previous works have shown that Al–20 wt.%Zn alloy after deformation also possesses excellent strength and plasticity [27–29]. Thus, excellent mechanical properties and damping capacity may be simultaneously obtained in the Al–Zn systems.

Sauvage et al. [24] found that the volume fraction of Zn phase in the as-deformed Al–Zn alloys increased with increasing the Zn content. Compared with the Al–20Zn alloy, the Al–Zn alloys with higher Zn contents should contain more Zn phase and Al-Zn interfaces under the same deformation process. So, a better combination of the mechanical properties and damping capacities is expected to obtain in the Al–Zn alloys with higher Zn content.

In the present study, an Al–35 wt.%Zn alloy was rolled at different conditions to investigate the effects of grain size, PB and GB structures, precipitation, and dislocations on the damping capacity and mechanical properties of Al–Zn alloy. The aim is to fabricate Al alloys with excellent damping capacity and mechanical properties.

2. Experimental methods

The Al–35Zn alloy was prepared by melting the commercial pure Al (99.9%) and pure Zn (99.9%) in a resistance heating furnace with a graphite crucible. The as-cast alloy was solid solution treatment with 753 K for 5 h and consequently quenched in water (defined as SS). Rolling was conducted with three rolling procedures: 1) hot rolling from 12 to 6 mm for 6 passes (defined as 50 HR); 2) hot rolling from 12 to 1.2 mm for 10 passes (defined as 90 HR); 3) hot rolling from 12 to 6 mm for 6 passes and subsequently cold rolling to 1.2 mm for 4 passes at room temperature (defined as 50 HR + 80 CR). The hot rolling temperature was controlled at approximately 733 K and the samples were reheated in a furnace at 733 K for 5 min between every hot rolling pass.

The microstructures of the samples were examined by optical microscopy (OM) and transmission electron microscopy (TEM, JEM-2010). The films for TEM were prepared by grinding to a thickness of 50 μm, followed by thinning using a twinjet electropolishing device in a solution of 5 vol% acetic acid and 95 vol% methanol at room temperature. The voltage was 10–15 V. The internal friction behavior (i.e., damping performance) together with the dynamic modulus of the samples was characterized using specimens with a dimension of 1.2 mm × 4 mm × 25 mm. Internal friction tests were conducted by a dynamic mechanical analyzer (Q800, TA) in single-cantilever mode. Measurements were made at frequency (f) of 1–10 Hz, strain amplitudes (ε) of 3.5×10^{-3} to 1.8×10^{-1}, and temperatures (T) of 300–630 K with a heating rate of 5 K/min. Furthermore the temperature dependent damping of commercial Al alloys such as AA 7055-T6 and AA 5086-H112 were also characterized for comparison.

Tensile tests were conducted on an Instron 5982-type testing machine at a strain rate of 4×10^{-4} s^{-1}. All of the specimens for tensile test were machined parallel to the rolling direction. The tensile fracture surfaces were observed by scanning electron microscopy (SEM, S4800).

3. Results and discussion

Fig. 1 shows the OM microstructures of the Al–35Zn alloys after solid solution treatment and rolling. The equiaxed grains with an average grain size of approximately 170 μm were observed in the SS sample (Fig. 1a). All hot rolled samples exhibited elongated grains in the rolling direction, and the grain size decreased significantly as the rolling reduction increased (Fig. 1b and c). The average short axis size of the elongated grains in the 90 HR sample was approximately 35 μm (Fig. 1c). The grains in the 50 HR + 80 CR sample were difficult to identify by OM due to the appearance of a high density of cold rolling-induced shear bands (Fig. 1d).

Fig. 2 shows the TEM images of the Al–35Zn alloys after solid solution treatment and rolling. The microstructure of the SS sample was characterized by the low density of dislocations, well-defined GBs, absence of precipitates in the grain interior and certain residual Zn phases with a size of several hundred nanometers along the GBs (Fig. 2a). In the 50 HR sample, a high density of rod-like Zn phase with sizes below 30 nm was observed in the grain interior (Fig. 2b). Upon further increasing the hot rolling reduction to 90%, larger sizes of the precipitated Zn phases were observed (Fig. 2c). Compared with the hot rolled samples, the 50 HR + 80 CR sample exhibited significantly higher density of dislocations and finer Al grains with a size of hundreds of nanometers. Furthermore, some precipitated Zn phases were coarsened to as large as 200 nm, changed to an equiaxed shape and located at the triple junctions of the Al grains following cold rolling (Fig. 2d). Thus, more boundaries between Al and Zn phases were obtained in the 50 HR + 80 CR sample.

A dynamic precipitation was observed in the Al–35Zn alloy during rolling (Fig. 2). The Zn atoms exhibited high instability in the Al lattices under deformation [22–26], and the solid solution decomposition increased as the deformation degree increased [27,28]. Therefore, the size of the precipitated Zn phases in the 90 HR sample was larger than that in the 50 HR sample. In our previous study, it was discovered that, compared with heating, both the deformation-induced vacancies and dislocations could cause the movement of larger number of Zn atoms and consequently easy formation of the Zn phase [30].

Furthermore, the precipitated Zn particles tended to gather in the crystal defects such as subgrain boundaries and dislocations. Dynamic recrystallization led to continuous transformation of the subgrain boundaries to the high-angle GBs during cold rolling, and therefore some coarsened Zn particles with equiaxed shape were situated at the triple junctions of the Al grains [28]. In this case, the size of precipitated Zn phases and the boundaries between Al and Zn phases in the 50 HR + 80 CR sample were respectively larger and more than those in the 90 HR sample.

Fig. 3 shows the damping and storage modulus of the Al–35Zn alloys. The damping capacities of the Al–35Zn alloys were decreased with increasing frequency; this phenomenon was more obvious in the 50 HR + 80 CR sample (Fig. 3a). The numbers of mobile dislocations in alloys increased with decreasing frequency at a constant temperature and amplitude, because more pinned dislocations could be activated at the low frequency stress. Therefore, higher damping capacity was obtained during low-frequency vibration according to the Granato–Lücke model [12]. Compared with the SS and hot rolled samples, the 50 HR + 80 CR sample exhibited higher density of dislocations (Fig. 2), thus this sample showed a much higher damping capacity at the low frequency stress and more obvious decline of damping capacity with increasing frequency.

The damping capacities of the Al–35Zn alloys were increased with increasing strain amplitude, and the damping capacity of 50 HR + 80 CR sample were higher than that of other samples in all strain amplitudes (Fig. 3b). Based on the Granato–Lücke model [12], solute atoms which are defined as weak pinning points, can effectively pin the dislocation segments at low vibration amplitude. Increasing the strain amplitude, dislocation segments break away

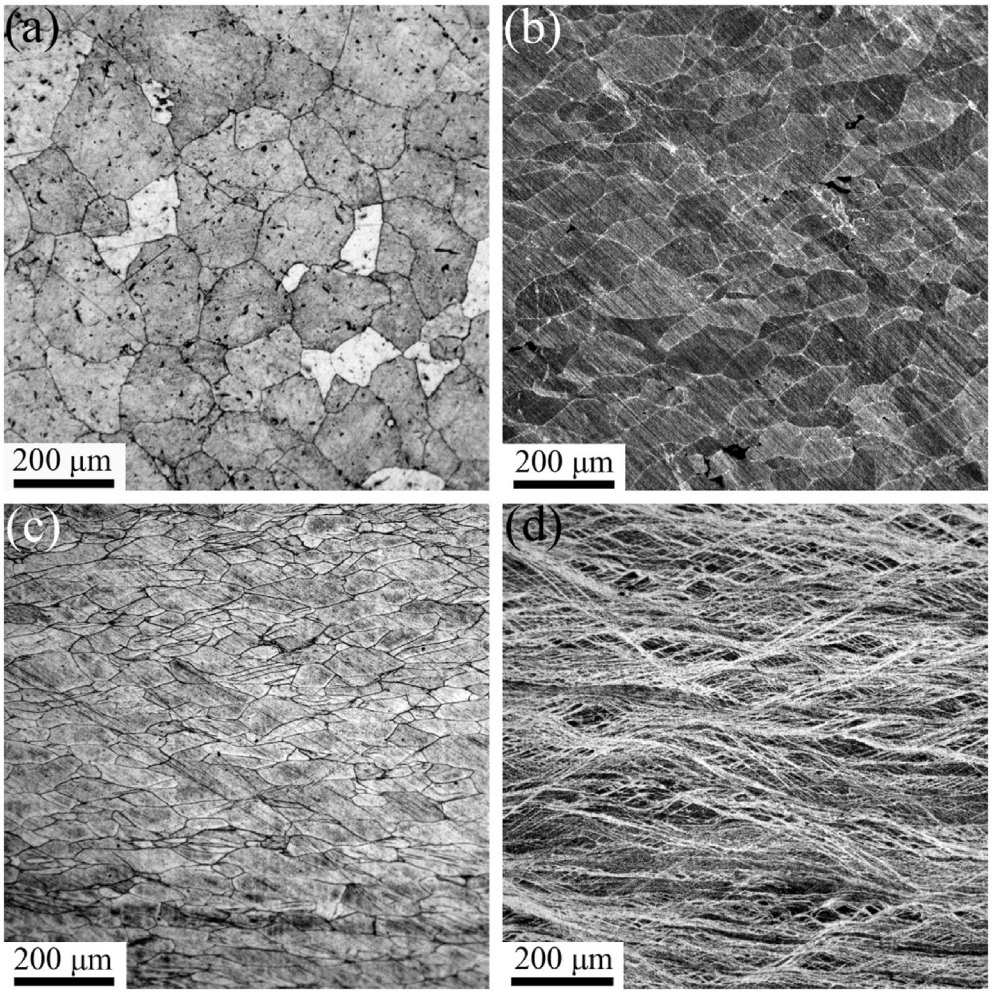

Fig. 1. OM images of various Al–35Zn samples: (a) SS, (b) 50 HR, (c) 90 HR, and (d) 50 HR + 80 CR.

from the weak pinning points but are still pinned by precipitates, which are defined as strong pinning points. So increasing strain amplitude, more pinned dislocations in the Al–35Zn alloys could be activated, and higher damping capacity was obtained.

Large number of Zn atoms in the Al lattice was consumed by dynamic precipitation during cold rolling. So, compared with the SS and hot rolled samples, the 50 HR + 80 CR sample exhibited less weak pinning points, and higher damping capacity at low strain amplitude. High density of GBs was obtained in the 50 HR + 80 CR sample due to the grain refinement. Similar to the dislocations, GBs as a crystal lattice defect can also contribute to the damping properties. Once the strain amplitude exceeds a critical value, the vibration of GBs occurs, resulting in increased internal friction. Therefore, the 50 HR + 80 CR sample also exhibited excellent damping capacity at high strain amplitudes.

Fig. 3c shows the variation of damping capacity with temperature for Al–35Zn alloys. The damping capacity was improved with increasing temperature because the viscous flow at PBs or GBs would convert mechanical energy into thermal energy as a result of internal friction at PBs or GBs [31].

Rolling can obviously improve the damping capacity of Al–35Zn alloys at both low and high temperatures. The damping peak height of the 50 HR + 80 CR sample was significantly higher than that of other samples. As shown in Figs. 1 and 2d, the ultrafine Al grains with a size below 1 μm were obtained in the 50 HR + 80 CR sample. The fine grain structure always contributes to excellent GB sliding capacity [2]. Therefore, the temperature-dependent damping capacities of Al–35Zn alloys were improved by rolling according to interfacial damping mechanism.

The interface between Al and Zn phases has been proven to own a well wettability, and the PB sliding capacities of Zn-Al and Al-Zn can be improved by those special wetting interface [15,20,21,32]. So, the Zn-Al alloys exhibited well high-temperature damping property [15,20,21]. In the present study, the Al-Zn interface was also observed in the 50 HR + 80 CR sample (Fig. 2d). Furthermore, it was also found that the thin Zn layers could be developed between the Al grains in the Al-20Zn alloy during cold rolling in our previous study [29]. Valiev et al. [32] demonstrated that the GB sliding capacity of Al-Zn alloys could be significantly improved by introducing Zn phase between the Al/Al GBs. Thus, the 50 HR + 80 CR sample exhibited the best temperature-dependent damping capacity.

The damping peaks in the 50 HR, 90 HR, and 50 HR + 80 CR samples were observed at temperatures about 630 K, 590 K, and 575 K, respectively. No peak was observed in the SS sample (Fig. 3c). The damping peak temperature in the 50 HR sample approximately corresponds to about the recrystallization temperature (0.6 *Tm*) of the Al–35Zn alloy. So the damping peaks in the Al–35Zn alloys were caused by the recrystallization. A similar phenomenon was also observed in the Zn–Al alloys [15,20,21]. The decrease of damping peak temperatures in the 90 HR and 50 HR + 80 CR samples can be attributed to the grain refinement, which can

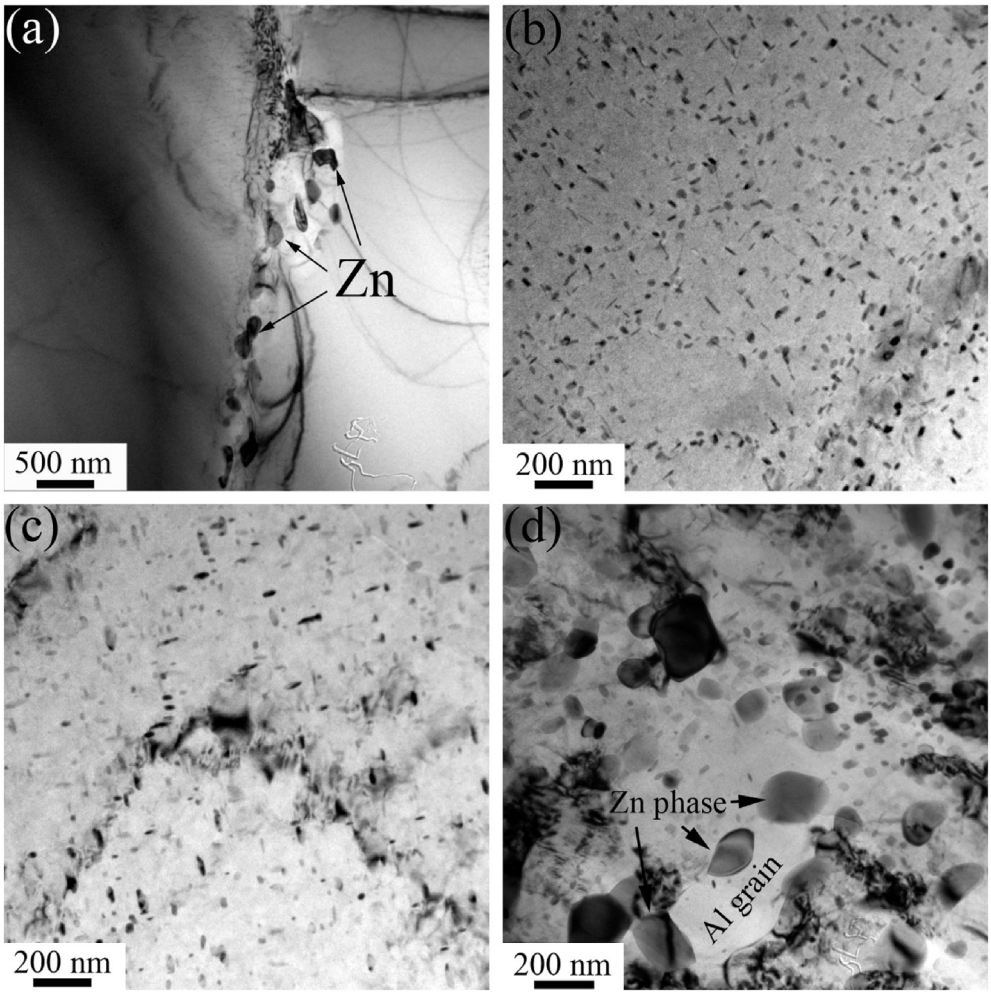

Fig. 2. TEM images of (a) SS, (b) 50 HR, (c) 90 HR, and (d) 50 HR + 80 CR Al–35Zn alloys.

reduce the recrystallization temperature.

Fig. 4 shows the comparison of temperature dependent damping between Al-35Zn alloys and some commercial Al alloys such as AA 7055-T6 and AA 5086-H112. The SS sample exhibited nearly similar damping property with those of the commercial Al alloys. While the damping property of the 50 HR + 80 CR sample were significantly higher than those of the commercial Al alloys due to the higher GB sliding capacity in the 50 HR + 80 CR sample. Table 1 summarizes the internal friction (IF) of SS, 90 HR, 50 HR + 80 CR samples and other high damping Al alloys and Al matrix composites (AMMCs), based on literature data [6,21,33,34]. The damping capacity of the SS sample was slightly lower that of the AMMCs. The 90 HR exhibited a significantly improved damping capacity, and the value was close to the IF of the Al-78Zn alloy, which was regarded as a high damping material [15,21]. For all of the Al alloys or AMMCs, the 50 HR + 80 CR sample exhibited highest IF value. So cold rolling is an effective method to improve the damping capacity of Al alloy.

The storage modulus values of the rolled Al–35Zn alloys decreased, until reach to their damping peak temperatures, and then increased with increasing the temperature (Fig. 3d). The increased storage modulus at high temperatures could be attributed to the dissolution of Zn atoms into Al lattice in the rolled Al–35Zn alloys at high temperature damping test.

The stress–strain curves of the rolled Al–35Zn alloys are compared in Fig. 5. Compared with the 50 HR sample, the 90 HR sample exhibited similar strength, but a significantly higher ductility. The ultimate tensile strength (UTS) and tensile elongation (EL) of the 90 HR sample reached up to 401 MPa and 9.6%, respectively. Compared with the 90 HR sample, the 50 HR + 80 CR sample exhibited higher strength, but a significantly lower ductility. The UTS and EL of this sample reached to 422 MPa and 4.6%, respectively.

The hot rolling reduction increase from 50% to 90% did not change the strength of the rolled Al–35Zn alloy. A microstructural analysis demonstrated the two competing effects of the further hot rolling on the strength of the Al–35Zn alloy: (i) hardening by grain refinement; and (ii) softening by coarsening of the nano-sized Zn phases and the decomposition of the Al–Zn solid solution. The net effect resulted in almost unchanged strength of Al–35Zn alloy during the further hot rolling. The cold rolled Al–35Zn alloy exhibited the highest strength, mainly attributed to the higher density of dislocations and finer grains (Fig. 2d).

The tensile fracture surfaces of the rolled Al–35Zn alloys are presented in Fig. 6. The 50 HR sample presented an intergranular brittle fracture with partial dimple gliding features. The casting defect such as crack was also observed in this sample (Fig. 6a). Therefore, the 50 HR sample exhibited a low ductility.

The GBs and large numbers of dimples were observed on the fracture surfaces of the 90 HR sample (Fig. 6b). So the rupture model of this sample consists of intergranular and transgranular fractures. A microstructural analysis demonstrated the two effects

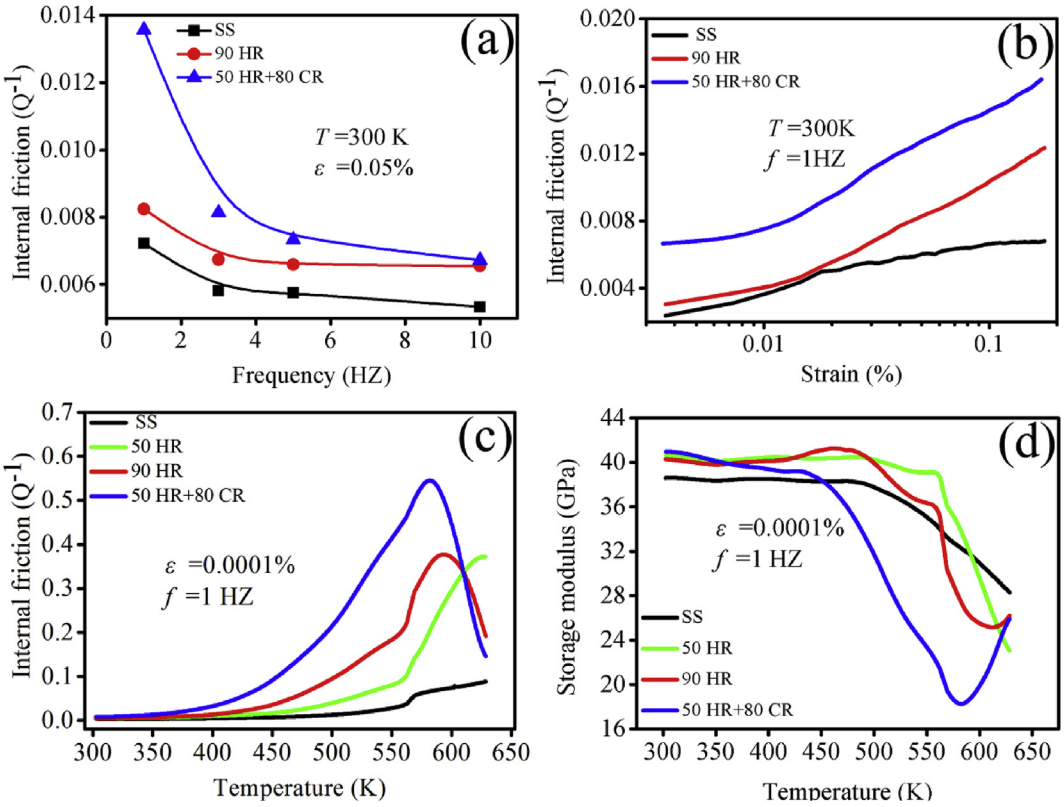

Fig. 3. (a) Frequency, (b) strain amplitude, and (c) temperature dependent damping, and (d) temperature dependent storage modulus of Al–35Zn alloys after solid solution treatment and different rolling processes.

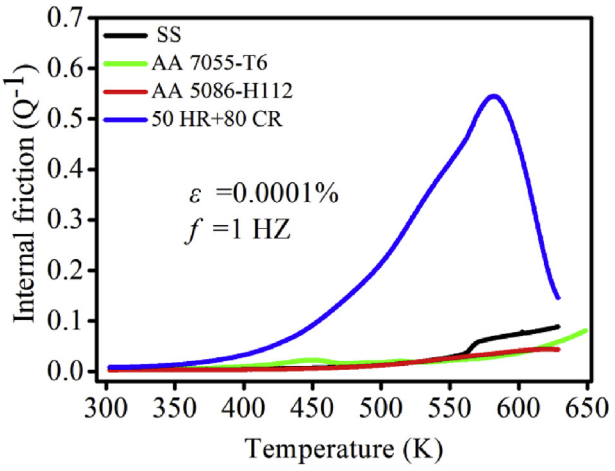

Fig. 4. Comparison of temperature dependent damping between Al-35Zn alloys and the commercial Al alloys such as AA 7055-T6 and AA 5086-H112 alloys.

of further hot rolling on the ductility of the Al–35Zn alloy. First, increasing rolling reduction led to that the grains of the Al–35Zn alloy were significantly elongated along the rolling direction, and shortened with respect to the normal direction (Fig. 1). The tensile direction was parallel to the rolling direction, and the length of single GB, which was parallel to the crack propagation direction during tension, in the 90 HR sample was much shorter than that in the 50 HR sample. Thus, the crack propagation along GBs was suppressed in the Al–35Zn alloy, and the ductility of this sample was improved after further hot rolling. Second, increasing rolling reduction led to that the casting defects, which could act as preferential sites for crack nucleation and preferential crack propagation path during the tensile process, were further eliminated in the Al–35Zn alloy. Thus, the plastic instability and the onset of necking of Al–35Zn alloy were suppressed after further hot rolling.

Table 1
Comparison of IF of Al–35Zn alloys with other high damping Al alloys or AMMCs at 1 Hz and 523 K.

	IF (Q^{-1})	ε (%)	References
AA8090-12%SiC	0.078	–	[33]
AA2519-11%SiC	0.02	–	[33]
AA6061-10%SiC	0.04	–	[33]
A356	0.026	0.005	[34]
Al-11Si-2CNT-5SiC	0.078	–	[6]
Al-78Zn	0.17	0.0001	[21]
SS	0.02	0.0001	This work
90 HR	0.137	0.0001	This work
50 + 80 CR	0.306	0.0001	This work

The ductile rupture was also observed in the 50 HR + 80 CR sample (Fig. 6c). The elongated grains were broken and recrystallized grains were observed in the 50 HR + 80 CR sample (Figs. 1d and 2d). So, the intergranular fracture of the Al–35Zn alloy was further suppressed by grain refinement after cold rolling. The depth of the dimples in the 50 HR + 80 CR sample was much smaller than that in the 90 HR sample, which corresponds to the lower EL. The structural characteristics with both the high density of dislocations and the fine grains always led to a low dislocation accumulation capability during tension [33–37], therefore the cold rolled Al–35Zn alloy exhibited both a low work hardening capability and low ductility.

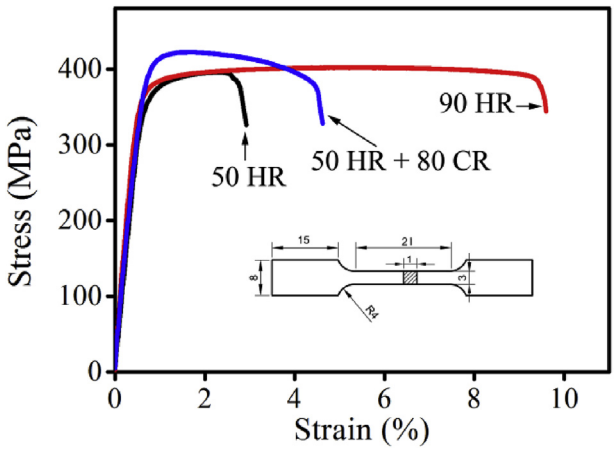

Fig. 5. Stress–strain curves of Al–35Zn alloys produced with various rolling parameters. The inset is the dimension and shape of tensile specimen.

and mechanical properties of this alloy. The following conclusions are reached:

(1) The average grain size of Al–35Zn alloy decreased with the increase of rolling reduction. The nano-sized Zn particles with a rod-like shape were precipitated during hot rolling. The cold rolling led to the formation of ultrafine Al grains, and the precipitated Zn phases were coarsened to hundreds of nanometers with an equiaxed shape, which were located at the triple junctions of the Al grains.
(2) The room/high-temperature damping capacities of the Al–35Zn alloy were simultaneously improved by cold rolling. This phenomenon was mainly attributed to the special microstructure characterized by fine grain structure, low solid solubility, and special wetting interface between Al and Zn phases in the cold rolled sample.
(3) The 50 HR + 80 CR sample demonstrated a high tensile strength of 422 MPa, with the main strengthening mechanisms being work hardening by the high density of dislocations and boundary strengthening by the grain refinement.
(4) The 90 HR sample showed balanced mechanical properties, including an enhanced strength and a reasonable ductility. The main strengthening mechanisms of this alloy included

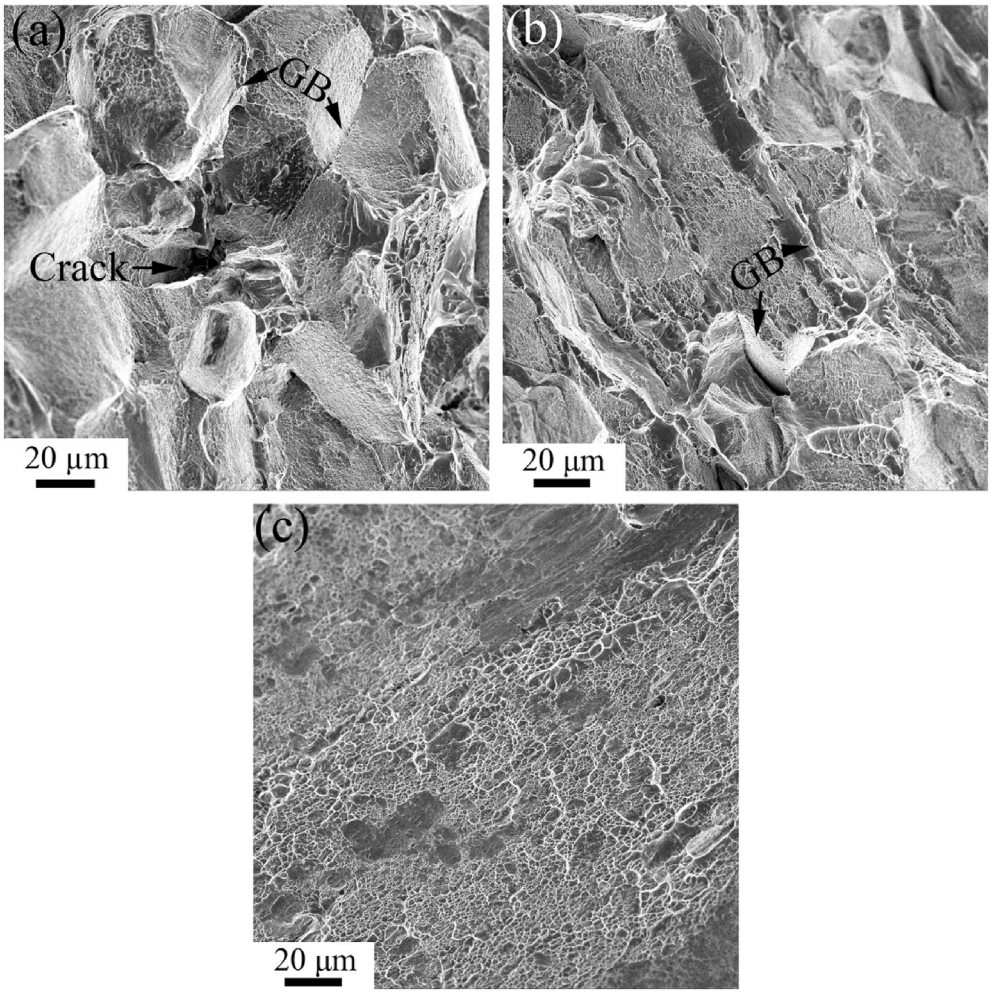

Fig. 6. Fracture surfaces of (a) 50 HR, (b) 90 HR, and (c) 50 HR + 80 CR Al–35Zn alloys.

4. Conclusions

In this study, the binary Al–35Zn alloy was rolled at different conditions to investigate the effects of grain size, PB and GB structures, precipitation, and dislocations on the damping capacity

precipitation strengthening by the high density of nano-sized Zn particles and boundary strengthening by the grain refinement.

Acknowledgements

This work was funded by National Natural Science Foundation of China (No. 51465014), the Guangxi 'Bagui' Teams for Innovation and Research, and Guangxi Natural Science Foundation (No. 2015GXNSFBA139238), National Basic Research Program of China (No. 2013CB733000).

References

[1] B.S. Yan, X.P. Dong, R. Ma, S.Q. Chen, Z. Pan, H.J. Ling, Mater. Sci. Eng. A 594 (2014) 168–177.
[2] F.C. Liu, Z.Y. Ma, F.C. Zhang, J. Mater. Sci. Technol. 28 (2012) 1025–1030.
[3] M.C. Gui, D.B. Wang, J.J. Wu, G.J. Yuan, C.G. Li, Mater. Sci. Eng. A 286 (2000) 282–288.
[4] N. Srikanth, H.K.F. Calvin, M. Gupta, Mater. Sci. Eng. A 423 (2006) 189–191.
[5] D.R. Ni, J.J. Wang, Z.Y. Ma, J. Mater. Sci. Tech. 32 (2016) 162–166.
[6] O. Carvalho, G. Miranda, M. Buciumeanu, M. Gasik, F.S. Silva, S. Madeira, Comp. Struct. 141 (2016) 155–162.
[7] S. Madeira, G. Miranda, V.H. Carneiro, D. Soares, F.S. Silva, O. Carvalho, Mater. Des. 93 (2016) 409–417.
[8] Y.J. Zhang, N.H. Ma, H.W. Wang, Mater. Lett. 61 (2007) 3273–3275.
[9] C.D. Lee, Mater. Sci. Eng. A 394 (2005) 112–116.
[10] E.J. Lavernia, R.J. Perez, J. Zhang, Metall. Mater. Trans. A 26A (1995) 2803–2818.
[11] P.Y. Li, H.J. Yu, S.C. Chai, Y.R. Li, Scr. Mater. 49 (2003) 819–824.
[12] G.Y. Xie, R. Schaller, C. Jaquered, Mater. Sci. Eng. A 252 (1992) 78–84.
[13] Z.Y. Zhang, X.Q. Zeng, W.J. Ding, Mater. Sci. Eng. A 392 (2005) 150–155.
[14] X.S. Hu, K. Wu, M.Y. Zheng, Scr. Mater. 54 (2006) 1639–1643.
[15] B.H. Luo, Z.H. Bai, Y.Q. Xie, Mater. Sci. Eng. A 370 (2004) 172–176.
[16] F.C. Liu, Z.Y. Ma, L.Q. Chen, Scr. Mater. 60 (2009) 968–971.
[17] Z.Y. Ma, F.C. Liu, R.S. Mishra, Acta Mater. 58 (2010) 4693–4704.
[18] Z.Y. Ma, S.R. Sharma, R.S. Mishra, Scr. Mater. 54 (2006) 1623–1626.
[19] F.C. Liu, Z.Y. Ma, Scr. Mater. 59 (2008) 882–885.
[20] J.N. Wei, D.Y. Wang, W.J. Xie, J.L. Luo, F.S. Han, Phys. Lett. A 366 (2007) 134–136.
[21] Z.H. Ma, F.S. Han, J.N. Wei, J.C. Gao, Metall. Mater. Trans. A 32 (2001) 2657–2661.
[22] A. Alhamidi, K. Edalati, Z. Horita, S. Hirosawa, K. Matsuda, D. Terada, Mater. Sci. Eng. A 610 (2014) 17–27.
[23] C.Y. Liu, B. Zhang, P.F. Yu, R. Jing, M.Z. Ma, R.P. Liu, Mater. Sci. Eng. A 580 (2013) 36–40.
[24] X. Sauvage, M.Y. Murashkin, B.B. Straumal, E.V. Bobruk, R.Z. Valiev, Adv. Eng. Mater. 17 (2015) 1821–1827.
[25] B.B. Straumal, B. Baretzky, A.A. Mazilkin, F. Phillipp, O.A. Kogtenkova, M.N. Volkov, R.Z. Valiev, Acta Mater. 52 (2004) 4469–4478.
[26] A.A. Mazilkin, B.B. Straumal, E. Rabkin, B. Baretzky, S. Enders, S.G. Protasova, O.A. Kogtenkova, R.Z. Valiev, Acta Mater. 54 (2006) 3933–3939.
[27] C.Y. Liu, M.Z. Ma, R.P. Liu, K. Luo, Mater. Sci. Eng. A 654 (2016) 436–441.
[28] C.Y. Liu, L. Yu, M.Z. Ma, R.P. Liu, Z.Y. Ma, Philos. Mag. Lett. 95 (2015) 539–546.
[29] C.Y. Liu, B. Qu, Z.Y. Ma, M.Z. Ma, R.P. Liu, Mater. Sci. Eng. A 657 (2016) 284–290.
[30] C.Y. Liu, H.J. Jiang, C.X. Wang, H.Q. Qi, Y.B. Li, M.Z. Ma, R.P. Liu, Chin. Phys. Lett. 33 (2016) 056101.
[31] H. Watanabe, T. Mukai, M. Sugioka, K. Ishikawa, Scr. Mater. 51 (2004) 291–295.
[32] R.Z. Valiev, M.Y. Murashkin, A. Kilmametov, B. Straumal, N.Q. Chinh, T.G. Langdon, J. Mater. Sci. 45 (2010) 4718–4724.
[33] R. Bauri, M.K. Surappa, Metall. Mater. Trans. A 36 (2005) 667–673.
[34] Y.J. Zhang, N.H. Ma, H.W. Wang, X.F. Li, Mater. Des. 29 (2008) 706–708.
[35] I. Sabirov, M.Yu. Murashkin, R.Z. Valiev, Mater. Sci. Eng. A 560 (2013) 1–24.
[36] H.L. Jia, R. Bjørge, K. Marthinsen, Y.J. Li, J. Alloy. Comp. 697 (2017) 239–248.
[37] H.H. Ktari, J.P. Couzinie, J. Bourgon, Y. Champion, N. Njah, J. Alloy. Comp. 647 (2015) 152–158.